Vegetation biomass change in China in the 20th century: an assessment based on a combination of multi-model simulations and field observations

Xiang Song, Fang Li, Sandy Harrison, Tianxiang Luo, Almut Arneth, Matthew Forrest, Stijn Hantson, Gitta Lasslop, Stephane Mangeon, Jian Ni, et al.

Vegetation biomass change in China in the 20th century: an assessment based on a combination of multi-model simulations and field observations

To cite this article: Xiang Song *et al* 2020 *Environ. Res. Lett.* **15** 094026

Environmental Research Letters

LETTER

Vegetation biomass change in China in the 20th century: an assessment based on a combination of multi-model simulations and field observations

Xiang Song[1], Fang Li[1,16], Sandy P Harrison[2,3], Tianxiang Luo[4], Almut Arneth[5], Matthew Forrest[6], Stijn Hantson[7,5], Gitta Lasslop[6], Stephane Mangeon[8,9], Jian Ni[10], Chao Yue[11,12], Thomas Hickler[6], Yiqi Luo[13], Stephen Sitch[14], Xin Xu[1] and Zaichun Zhu[15]

[1] International Center for Climate and Environment Sciences, Institute of Atmospheric Physics, Chinese Academy of Sciences, Beijing, People's Republic of China
[2] School of Archaeology, Geography & Environmental Science, Reading University, Reading, United Kingdom
[3] Department of Earth System Science, Tsinghua University, Beijing, People's Republic of China
[4] Institute of Tibetan Plateau Research, Chinese Academy of Sciences, Beijing, People's Republic of China
[5] Karlsruhe Institute of Technology, Institute of Meteorology and Climate research, Atmospheric Environmental Research, Garmisch-Partenkirchen, Germany
[6] Senckenberg Biodiversity and Climate Research Centre (BiK-F), Senckenberganlage, Germany
[7] Geospatial Data Solutions Center, University of California, Irvine, CA, United States of America
[8] Department of Physics, Imperial College London, London, United Kingdom
[9] Now at CSIRO, Data61, Brisbane, QLD, Australia
[10] Zhejiang Normal University, Jinhua, Zhejiang, People's Republic of China
[11] State Key Laboratory of Soil Erosion and Dryland Farming on the Loess Plateau, Northwest A&F University, Yangling, Shanxi, People's Republic of China
[12] Laboratoire des Sciences du Climatet de l'Environnement, LSCE/IPSL, CEA-CNRS-UVSQ, Université Paris-Saclay, France
[13] Department of Biological Sciences, Northern Arizona University, Flagstaff, AZ, United States of America
[14] College of Life and Environmental Sciences, University of Exeter, Exeter, United Kingdom
[15] School of Urban Planning and Design, Peking University Shenzhen Graduate School, ShenZhen, People's Republic of China
[16] Author to whom any correspondence should be addressed.

E-mail: lifang@mail.iap.ac.cn

OPEN ACCESS

RECEIVED
18 November 2019

REVISED
19 April 2020

ACCEPTED FOR PUBLICATION
20 May 2020

PUBLISHED
21 August 2020

Keywords: vegetation biomass, China, 20th century changes, land use and land cover change, climate change, CO_2 concentration, DGVM simulations

Supplementary material for this article is available online

Abstract

Vegetation biomass is a key and active component of the carbon cycle. Though China's vegetation biomass in recent decades has been widely investigated, only two studies have quantitatively assessed its century-scale changes so far and reported totally opposite trends. This study provided the first multi-model estimates of China's vegetation biomass change for the 20th century and its responses to historical changes in environmental and anthropogenic factors, based on simulations evaluated with the field observations from 3757 inventory plots in China and bias-corrected using machine learning (Gaussian process regression). A significant decline in vegetation biomass over the 20th century was shown by bias-corrected simulations from the six Dynamic Global Vegetation models (DGVMs) with trends ranging from −32.48 to −11.10 Tg C yr^{-1} and a mean trend of −17.74 Tg C yr^{-1}. Land use and land cover change (LULCC) was primarily responsible for the simulated downward trend (−50.71 to −24.28 Tg C yr^{-1}), while increasing atmospheric CO_2 concentration lead to increased vegetation biomass (+9.27 to + 13.37 Tg C yr^{-1}). Climate change had limited impacts on the long-term trend (−3.75 to + 5.06 Tg C yr^{-1}). This study highlights the importance of LULCC for historical reconstruction and future projection of vegetation biomass over China. It also suggests that the incorrect change in China's forest area for 1980–2000 in the LULCC dataset used as model input data of many existing and ongoing model intercomparison projects (MIPs) has likely led to inaccurate estimations of historical vegetation biomass changes in China.

1. Introduction

China is the most populous country and the largest carbon emitter in the world, and has undergone distinct land-use and climate changes during the 20th century (Fang *et al* 2018). Assessment of vegetation biomass and its change over China is essential for understanding the regional, and even the global, carbon cycle (Kondo *et al* 2013, Fang *et al* 2018).

Many studies have estimated China's vegetation biomass in recent decades using various approaches. Estimates of present-day vegetation biomass in China range from 13.34 to 35.23 Pg C based on numerical models (Li *et al* 2004, Ni 2001, and references therein), and from 13.09 to 34.68 Pg C based on field and satellite observations (Carvalhais *et al* 2014, Li *et al* 2015, Xu *et al* 2018, Fang *et al* 2018; and references therein). Fang *et al* (2018) and Tang *et al* (2018) estimated that forests, grasslands, shrublands, and croplands contributed to 80%, 10%, 5%, and 4% of current vegetation biomass, respectively, using extrapolation from site-level field observations based on a land cover map estimate. Xu *et al* (2018) investigated the spatial changes of 2004–2014 vegetation biomass by collecting data based on literature review, and concluded that mean annual precipitation is an important driver of the spatial changes. Several studies reported that vegetation biomass increased after ~1980 probably as a result of forest expansion and regrowth (Fang *et al* 2001, 2007, Tang *et al* 2018).

However, until now, only Wang *et al* (2007) and Mao *et al* (2009) have investigated the long-term change of China's vegetation biomass over the 20th century. Both studies were based on a single model, specifically, the Integrated Terrestrial Ecosystem C-budget model (InTEC) in Wang *et al* (2007) and a modified version of the Sheffield Dynamic Global Vegetation Model (SDGVM) in Mao *et al* (2009). The two studies reported opposite trends: China's vegetation biomass for the 20th century was decreased by 2.15 Pg C from Wang *et al* (2007) while increased by 2.07 Pg C from Mao *et al* (2009).

Historical changes in vegetation biomass are regulated by climate, atmospheric CO_2 concentration, and land use and land cover change (LULCC) (Kim *et al* 2017, Fang *et al* 2018, Xin *et al* 2018). Dynamic Global Vegetation Models (DGVMs) simulate the response of global terrestrial ecosystems to these drivers, and integrate biogeochemistry, biogeophysics, and vegetation dynamics at the land surface within a physically and chemically consistent modelling framework (e.g. Foley *et al* 1996; Sitch *et al* 2003). They can be used to isolate how each driver affects vegetation biomass, providing that the models produce (or can be induced to produce via bias correction) realistic simulations of the modern state (Piao *et al* 2011, Ichii *et al* 2013, Chen *et al* 2016). However, up to now, there has been no attempt to evaluate vegetation biomass simulated by DGVMs or correct their simulation bias before applying them to investigate the historical changes and drivers of global and regional vegetation biomass. The latter is important given that DGVMs aim to model the global simulations with low spatial resolution and generally do not conduct regional optimization. Furthermore, although Mao *et al* (2009) found that atmospheric CO_2 concentration change was more important than changes in temperature and precipitation in explaining vegetation biomass change of the 20th century, there has been no study to investigate the potential impact of other drivers on the historical change.

In this study, we used simulations by six state-of-the-art, fire-enabled DGVMs which were run following the same protocol and the same forcing datasets. We evaluated these simulations using site-specific biomass data from 3757 inventory plots in China. Biases in each model simulation were statistically corrected using machine learning (Gaussian process regression, GPR). The bias-corrected simulations provided the first multi-model estimates of vegetation biomass for the 20th century. We then used three sensitivity experiments in which potential drivers of 20th century vegetation changes, specifically, climate, CO_2 concentration and land-use, were constant, respectively, throughout the historical period to analyze the causes of the simulated changes in vegetation biomass.

2. Data and methods

2.1. Model simulations

We used vegetation simulations performed as part of the Fire Model Intercomparison Project (FireMIP, Hantson *et al* 2016, Rabin *et al* 2017) from six state-of-the-art fire-enabled DGVMs: CLM4.5 with an updated fire module for CLM5 (CLM4.5), JULES-INFERNO (JULES), JSBACH-SPITFIRE (JSBACH), LPJ-GUESS-SPITFIRE (LPJ-GS), LPJ-GUESS-SIMFIRE-BLAZE (LPJ-GSB), and ORCHIDEE-SPITFIRE (ORCHIDEE). The distribution of natural vegetation was simulated in JULES, LPJ-GS, and LPJ-GSB, but prescribed in the others. Only CLM4.5 and LPJ-GSB simulated an interactive nitrogen cycle (table 1). All the DGVMs are not stochastic except for LPJ-GUESS. LPJ-GUESS includes stochastic representation of individual establishment, mortality, and disturbance impacts. This does not affect the interpretability of the results because the simulations used here feature sufficient (50 for LPJ-GS and 25 for LPJ-GSB) replications so that the effect of the stochastic variability is small and the effect of drivers is dominant.

All the DGVM simulations started from a spin-up simulation for 1700 conditions to get the initial fields for subsequent 1701–2013 simulations (figure 1, see Rabin *et al* 2017 for details). For the spin-up runs, models were recycled until carbon values in the slowest soil carbon pool varied by less than 1%

Table 1. Summary description of the Dynamic global vegetation models (DGVMs) used in this study.

DGVM	DGVM description	Nat. veg. distribution[a]	N impact	References
CLM4.5	NCAR Community Land Model version 4.5 with C/N biogeochemical module, and updated fire module for CLM5	prescribed	N cycle	Oleson *et al* (2013) Li *et al* (2012, 2013) Li and Lawrence (2017)
JSBACH-SPITFIRE (JSBACH)	Jena Scheme for Biosphere-Atmosphere Coupling in Hamburg	prescribed	No	Brovkin *et al* (2013) Reick *et al* (2013) Lasslop *et al* (2014)
JULES-INFERNO (JULES)	Joint UK Land Environment Simulator, including INFERNO fire module	modeled	No	Best *et al* (2011) Clark *et al* (2011) Mangeon *et al* (2016)
LPJ-GUESS -SIMFIRE—BLAZE (LPJ-GSB)	Updated version of LPJ-GUESS model, with Blaze-Induced Land-Atmosphere Flux Estimator and the SIMple FIRE model	modeled	N cycle	Smith *et al* (2014) Knorr *et al* (2016)
LPJ-GUESS -SPITFIRE (LPJ-GS)	LPJ-GUESS with Spread and InTensity fire model (SPITFIRE)	modeled	No	Smith *et al* (2001) Ahlstrom *et al* (2012) Lehsten *et al* (2009)
ORCHIDEE -SPITFIRE (ORCHIDEE)	Organizing Carbon Hydrology In Dynamic EcosystEms	prescribed	No	Krinner *et al* (2005) Yue *et al* (2014 2015)

[a] 'nat. veg. distribution': spatial distribution of natural vegetation.

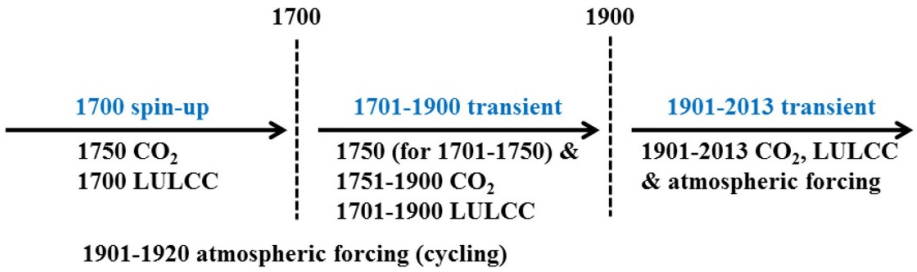

Figure 1. Experiment design for control simulation. The 1700 spin-up run is used to get the initial fields for subsequent transient simulations.

between consecutive 50 year periods for every grid cell. The atmospheric reanalysis data were from CRU-NCEP v5.3.2. Annual global atmospheric CO_2 concentration was derived from ice core and NOAA monitoring station data (Le Quéré *et al* 2014). LULCC data were from LUH1 (Hurtt *et al* 2011) in which changes in fractional coverage of croplands and pastures were from History Database of the Global Environment (HYDE) version 3.1 (Klein Goldewijk *et al* 2011, Klein Goldewijk and Verburg 2013). China's land use and land cover change in LUH1's LULCC data was characterized by expansion of croplands and a decrease in forest area in the 20th century (Liu and Tian 2010).

Sensitivity simulations were made to help understand the drivers of simulated changes in terrestrial ecosystems, including: (1) no climate change, (2) constant atmospheric CO_2 concentration, and (3) no LULCC (table 2, see Rabin *et al* 2017 for details). In the no climate change simulation, the climate throughout the run was the recycled time-varying 1901–1920 atmospheric forcing, but all other inputs were allowed to vary as in the simulation. In the constant CO_2 simulation, the atmospheric CO_2 concentration was held constant at 277.33 ppm for the whole of the simulation. In the no LULCC simulation, land cover in 1700 was used throughout the simulation.

All model outputs were converted to 1° spatial resolution, based on bilinear interpolation from low to high resolution for CLM4.5 (~1.9° latitude × 2.5° longitude), JSBACH (1.875°), and JULES (~1.2° latitude × 1.9° longitude), and on area-weighted averaging for those models with an original spatial resolution of 0.5°.

Not all of the FireMIP models were used in this study. LPJ-GUESS-GlobFIRM and LPJ-GUESS-SIMFIRE-BLAZE had the same vegetation model but used different fire models. Evaluation by Andela *et al* (2017) and Li *et al* (2019) showed that the fire model GlobFIRM simulated the global burned area and fire carbon emissions poorly. MC2 was developed for regional applications and applied globally without adequate calibration (Hantson *et al* 2019). An old version of CLASS-CTEM outputs did not complete all the sensitivity experiments (Li *et al* 2019), and

Table 2. Experiment design of control (CTRL) and three sensitivity simulations.

Exp. name	Climate	CO_2	LULCC
CTRL	Transient	Transient	Transient
S-CLIMATE	1901–1920 cycled[a]	Transient	Transient
S-CO_2	Transient	277.33 ppm	Transient
S-LULCC	Transient	Transient	Fixed at 1700 values

[a]Repeatedly cycling 1901–1920 atmospheric forcing (precipitation, temperature, specific humidity, surface pressure, wind speed, and solar radiation).

some bugs were identified in temporal variability of carbon fluxes and pools in its new version. Therefore, the simulations of the three models (LPJ-GUESS-GlobFIRM, MC2 and CLASS-CTEM) were excluded from our analyses.

2.2. Field observations

The field observations of vegetation biomass used here were collated and derived from Chinese forest survey inventories of Luo (1996) and Pan *et al* (2004) and from literature review (supplement B.xlsx and supplement B reference.docx). The vegetation biomass is derived as the sum of leaf, stem and branches, and root biomass or the sum of above-ground and below-ground biomass.

The dataset from Luo (1996) and Pan *et al* (2004) focused on forest plots, and provided information on location, forest type, and leaf, branch, stem, and root biomass for trees for all plots. It included 1266 forest plots, sampling tropical and monsoon forests, subtropical evergreen broadleaf and coniferous forests, temperate deciduous broadleaf forests, boreal evergreen/deciduous coniferous forests where the measurements were made on forests aged from 3 to 350 years during 1956–1993. Most of the organ biomass (leaf, branch and stem, root) was obtained by the biomass allometric growth model method. Missing values of tree roots were calculated from the ratio of above-ground to below-ground biomass of the same species in nearby stands (Luo 1996).

Furthermore, we compiled an additional dataset of above-/below- ground vegetation biomass for 1112 forest plots and 1379 grassland plots measured during 2000–2013 from published literature. We selected plots with observations of both above- and below-ground biomass and a clear description of the functional types or species. Observations in the literature were mainly obtained by the clear-cutting method, average standard tree method, and/or biomass allometric growth method. A coefficient of 0.45 was used to convert vegetation biomass density to C density (kg C m^{-2}) (e.g. Xu *et al* 2018).

2.3. Bias correction for vegetation biomass

To derive bias-corrected outputs from each of the DGVMs, we built statistical models between the default (uncorrected) vegetation biomass simulations and observations of vegetation biomass (total vegetation biomass) as follows. First, according to the vegetation-type or species records in the field observations and the plant functional type (PFT) information in the model outputs, we sorted the observations and simulations into evergreen broad-leaf, deciduous broad-leaf, evergreen needle-leaf, and deciduous needle-leaf tree PFTs and grass (not separating C3 and C4) PFT. Second, simulations were temporally averaged to match the representative periods of observations. Third, we built statistical models based on simulation-observation pairs that belonged to the same PFT over all grid cells.

Three methods for bias correction were tested: first order linear regression:

$$\boldsymbol{B_{i,j,obs}} = a_{i,j,0} + a_{i,j,1} \times \boldsymbol{B_{i,j,uncorrected}} \quad (1)$$

cubic regression:

$$\boldsymbol{B_{i,j,obs}} = a_{i,j,0} + a_{i,j,1} \times \boldsymbol{B_{i,j,uncorrected}} + a_{i,j,2} \times \boldsymbol{B^2_{i,j,uncorrected}} + a_{i,j,3} \times \boldsymbol{B^3_{i,j,uncorrected}} \quad (2)$$

and machine learning (Gaussian process regression, GPR). Here, $a_{i,j,n}$ ($n = 0, .., 3$) was regression coefficient for the ith functional type of the jth model, $\boldsymbol{B_{i,j,obs}}$ and $\boldsymbol{B_{i,j,uncorrected}}$ were the spatial arrays of field observations and the default (uncorrected) model outputs, respectively. For the machine learning GPR, we used the GPR package of Matlab version 2018b. We carried out batch training based on the GPR model to optimize the parameters of kernel function (ardsquared exponential function). Hyperparameters were then determined by automatic hyperparameter optimization based on minimizing five-fold cross-validation loss.

We adopted the commonly-used leave-one-out cross-validation framework (LOOCV, Wilks 1995) to build and evaluate the statistical models based on the three bias-correction methods for preventing over-fitting. In LOOCV, one observation-simulation pair was left out as test set, and the statistical model was built by using remaining observation-simulation pairs ($n - 1$) as training set. Then, the bias-corrected simulation value was predicted with the statistical model and the independent left-out simulation (uncorrected) value. The process was repeated n times to obtain n bias-corrected simulation values. The correlation coefficient (R) and root mean square error (RMSE) between simulations and field

Table 3. Total vegetation biomass estimates (Pg C) of China for uncorrected and bias-corrected multi-model simulations.

Method	Period	Uncorrected	Bias-corrected	References
CLM4.5	2001–2010	26.96 ± 0.63	13.23 ± 0.31	this study
JSBACH	2001–2010	30.88 ± 0.25	15.47 ± 0.13	this study
JULES	2001–2010	15.56 ± 0.12	12.13 ± 0.10	this study
LPJ-GSB	2001–2010	14.65 ± 0.18	11.72 ± 0.15	this study
LPJ-GS	2001–2010	25.90 ± 0.28	11.73 ± 0.13	this study
ORCHIDEE	2001–2010	17.14 ± 0.09	10.57 ± 0.05	this study
MMEM[a]	2001–2010	21.85 ± 0.11	12.48 ± 0.06	this study
Literature review	2004–2014	14.6 ± 3.24		Xu *et al* (2018)
Field inventory & land cover map	2001–2010	13.09		Fang *et al* (2018)

[a]MMEM: multi-model ensemble mean

observations were used as skill scores (skill is higher with higher R and lower RMSE). We selected the method with highest cross-validation skill as the correction method for all models and functional types which was denoted as correction function *f*. Analyses of cross-validation skill (table S1 (available online at stacks.iop.org/ERL/15/094026/mmedia)) showed that machine learning GPR outperformed the first order linear and cubic regressions for all functional types and models except deciduous forest in JULES.

We derived the bias-corrected biomass simulations ($B_{i,j,k,corrected}$) for functional type i of model j in year k during 1950–2013 as:

$$B_{i,j,k,corrected} = f(B_{i,j,k,uncorrected}) \quad (3)$$

Then, the total vegetation biomass ratio between with and without bias-correction averaged during 1950–2000 was used as bias-correct coefficient to modify the mean total vegetation biomass in 2001–2010, as well as trend in vegetation biomass change in the 20th century. This method assumes that the statistical relationship between the multi-year average of DGVM simulations and field observations is constant.

3. Results

3.1. Evaluation and bias correction

The models simulated present-day vegetation biomass in China ranged from 14.65 ± 0.18 to 30.88 ± 0.25 Pg C, with a multi-model ensemble mean (MMEM) of 21.85 ± 0.11 Pg C (table 3). The simulated biomass from CLM4.5 (26.96 ± 0.63 Pg C), JSBACH (30.88 ± 0.25 Pg C) and LPJ-GS (25.90 ± 0.28 Pg C), and the MMEM (21.85 ± 0.11 Pg C) were up to more than twice the latest estimates based on extensive literature review (14.60 ± 3.24 Pg C) (Xu *et al* 2018) and on an observation campaign (13.09 Pg C) (Fang *et al* 2018) (table 3).

Before bias correction, all the DGVMs showed a systematic bias in simulated vegetation biomass for tree, and grass PFTs compared to observations (figures S1–2). Specifically, CLM4.5, JSBACH, and JULES overestimated the vegetation biomass for evergreen tree PFTs, while ORCHIDEE underestimated it. LPJ-GS and ORCHIDEE overestimated the vegetation biomass for deciduous tree PFTs (figure S1). All models tended to underestimate grass vegetation biomass (figure S2). Moreover, the spatial heterogeneity of vegetation biomass was considerably underestimated by JULES and LPJ-GSB for tree PFTs (figure S1) and by all models except for CLM4.5 for grass PFTs (figure S2).

The bias-corrected results showed a significant improvement compared to the default simulations (figure 2). The correlation coefficients between corrected simulations and observations were much higher than uncorrected ones, and the RMSE was also lower in the bias-corrected simulations. All correlation coefficients for bias-corrected simulations passed the Student's t-test at the 0.001 significance level, indicating that the bias-corrected simulations can reproduce China's vegetation biomass reasonably well. In addition, the bias-corrected simulations provided an estimate of China's vegetation biomass averaged for the period 2001–2010 ranging from 10.57 ± 0.05 to 15.47 ± 0.13 Pg C with a MMEM of 12.48 ± 0.06 Pg C (table 3), close to the latest estimates of 13.09 Pg C from Fang *et al* (2018) and 14.6 ± 3.24 Pg C in Xu *et al* (2018). The uncertainty (inter-model spread) in simulated vegetation biomass was reduced through bias correction: standard deviation of the multi-model simulations reduced from 6.89 to 1.70 Pg C.

Spatially, all the bias-corrected DGVM simulations and the MMEM consistently showed that the vegetation biomass increases from northwest to southeast, in agreement with field observations and Carvalhais *et al* (2014) (figure 3). Grass or shrub was simulated as the dominant vegetation with low biomass in northwestern China because of cold or dry conditions, while warm and wet conditions in southeastern China resulted in more forest coverage and high biomass, in accordance with Köppen-Geiger classifications. When compared with uncorrected simulations (figure S3), bias correction decreased vegetation biomass estimates mostly in southern China and Northeast China.

3.2. Historical changes over the 20th century

All the six DGVMs exhibited an overall decline in vegetation biomass over the 20th century for China

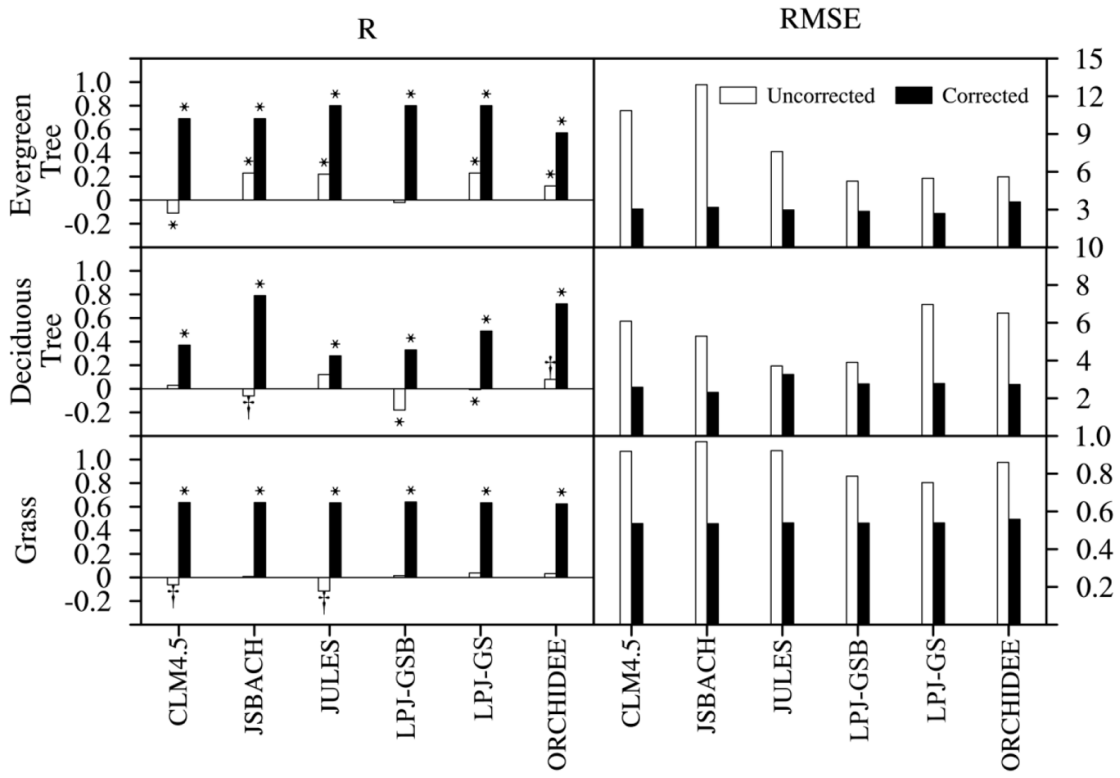

Figure 2. Comparison of correlation coefficient (R) and root mean square error (RMSE) between 1950–2000 and/ or 2000–2013 averaged PFT vegetation biomass (kg C (m^2 PFT area)$^{-1}$) from DGVM simulations with/without correction and field observations for evergreen and deciduous forests and grass in China. Simulations with higher R and lower RMSE is more skillful. R passed the Student's t-test at the 0.001 (*) or 0.1(†) significance level.

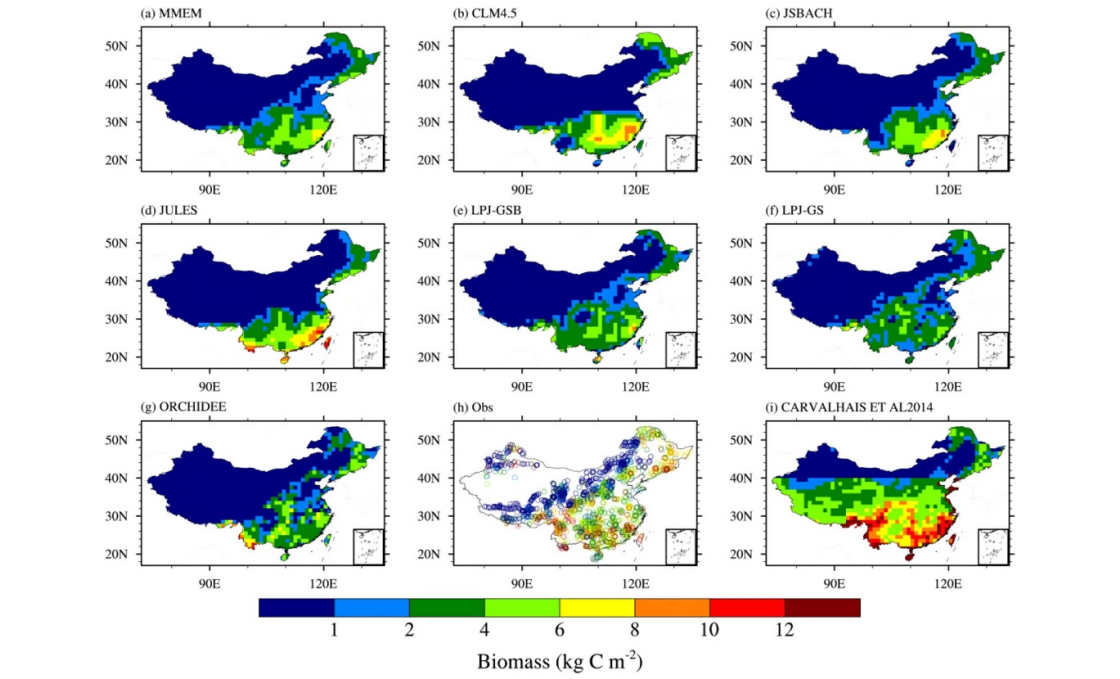

Figure 3. Spatial patterns of bias-corrected vegetation biomass (kg C m^{-2}) estimated by (a) MMEM of six DGVMs, (b)–(g) six DGVMs, (h) vegetation biomass observations over forest sites from Luo (1996) and literature review, and (i) estimates from Carvalhais *et al* (2014).

(significant at the 0.05 level using the Mann-Kendall test). The trends ranged from −32.48 Tg C yr^{-1} (LPJ-GS) to −11.10 Tg C yr^{-1} (JULES) (figure 4(a)). Only the ORCHIDEE model showed a different trajectory: biomass declined initially before the 1960 s and increased thereafter, with a trend of −17.51 Tg C yr^{-1}

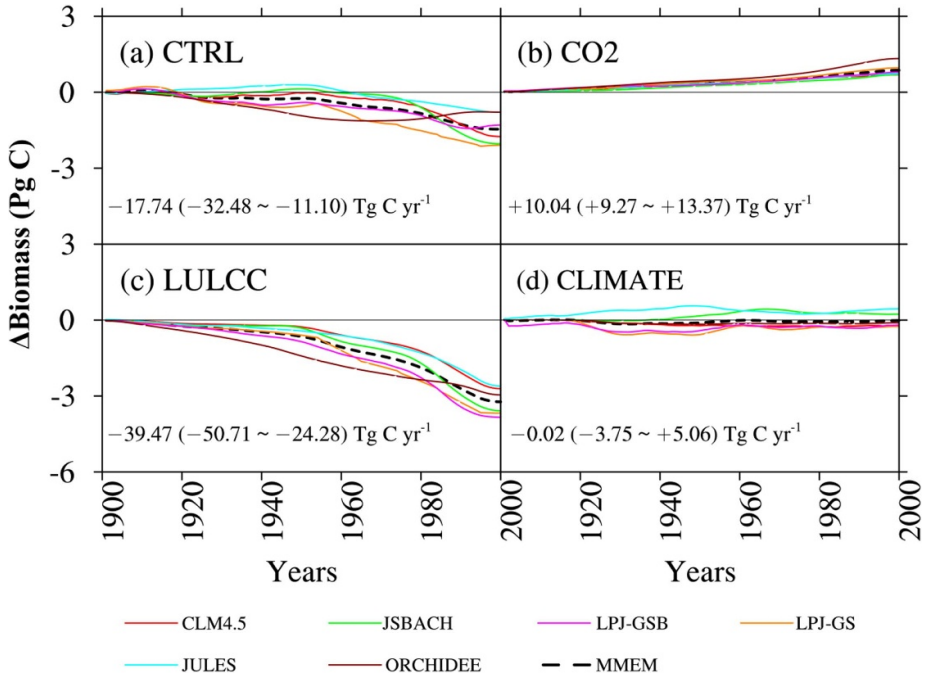

Figure 4. (a) Changes of China's total vegetation biomass (Pg C) for the 20th century (control simulation, CTRL) from bias-corrected simulations of six DGVMs and the MMEM, and their responses to (b) atmospheric CO_2 concentration change, (c) land use and land cover change (LULCC), and (d) climate change. An 11 year running mean is used. Trends of MMEMs and ranges of trends for individual DGVMs are also shown.

for the 20th century. The different change of ORCHIDEE after the 1960 s was caused by the stronger response to rising [CO_2] (figure 4(b)) partly due to no modeling of nitrogen limitation (table 1) and the weaker response to LULCC since the 1980 s (figure 4(c)) likely due to weaker decline in forest area (figure 6(a)) than other models. The MMEM of all DGVMs also exhibited a significant downward trend (–17.74 Tg C yr^{-1}).

All the DGVMs and MMEM agreed that rising [CO_2] between 1901 and 2000 tended to increase vegetation biomass. The trend ranged from + 9.27 Tg C yr^{-1} to + 13.37 Tg C yr^{-1}, with a trend of around + 10.04 Tg C yr^{-1} (figure 4(b)). Rising [CO_2] increased vegetation biomass over most regions of China (figure S4) probably because the models were constructed to respond to changes in [CO_2] by changing light absorption and light-use efficiency (Norby *et al* 2005, Mao *et al* 2009) and also changing forest water-use efficiency (Keenan *et al* 2013).

The model simulations for all the DGVMs and MMEM showed that LULCC decreased vegetation biomass over the 20th century (figure 4(c)). The effect of LULCC ranged from a strong decrease of −50.71 Tg C yr^{-1} for LPJ-GS to a moderate decrease of −24.28 Tg C yr^{-1} for JULES with an estimate of −39.47 Tg C yr^{-1} for the MMEM. LULCC impacts were the dominant driver for long-term changes in vegetation biomass over China for MMEM and all models (figure 4). Spatially, the largest impacts of LULCC on vegetation biomass were in the northeastern and southwestern forested regions (figure S5).

The impacts of climate change on the long-term trends of vegetation biomass were generally limited (figure 4(d)), with trends ranging from −3.75 Tg C yr^{-1} (CLM4.5) to + 5.06 Tg C yr^{-1} (JSBACH). There was no significant trend (at the 0.05 level) in the MMEM (–0.02 Tg C yr^{-1}). This was probably because the impacts of climate change over the 20th century are generally weak and have large spatial heterogeneity (figure S6).

The DGVM simulations without bias-correction exhibited similar trends in vegetation biomass and similar responses to the various drivers, but the downward trend and responses were stronger than those in the bias-corrected simulations (Figs. S7–11), partly because the magnitude of vegetation biomass was overestimated in the uncorrected simulations (table 1, figure S3). For example, the decline in the vegetation biomass over the 20th century in the uncorrected simulations ranged from −71.70 to −14.36 Tg C yr^{-1} (–31.81 Tg C yr^{-1} for MMEM) (figure S7), compared to trends of −32.48 to −11.10 Tg C yr^{-1} for bias-corrected simulations and −17.74 Tg C yr^{-1} for the MMEM (figure 4(a)).

The bias-corrected MMEM showed a significant decline in vegetation biomass over most of China for the 20th century, especially in the southwest (figure 5(a)). Only limited areas in northern China showed a slight increase in vegetation biomass. LULCC was the main reason for changes in vegetation biomass over 72.42% of China's land area (figure 5(b)), and largely driven by a decline in forest area. From 1901

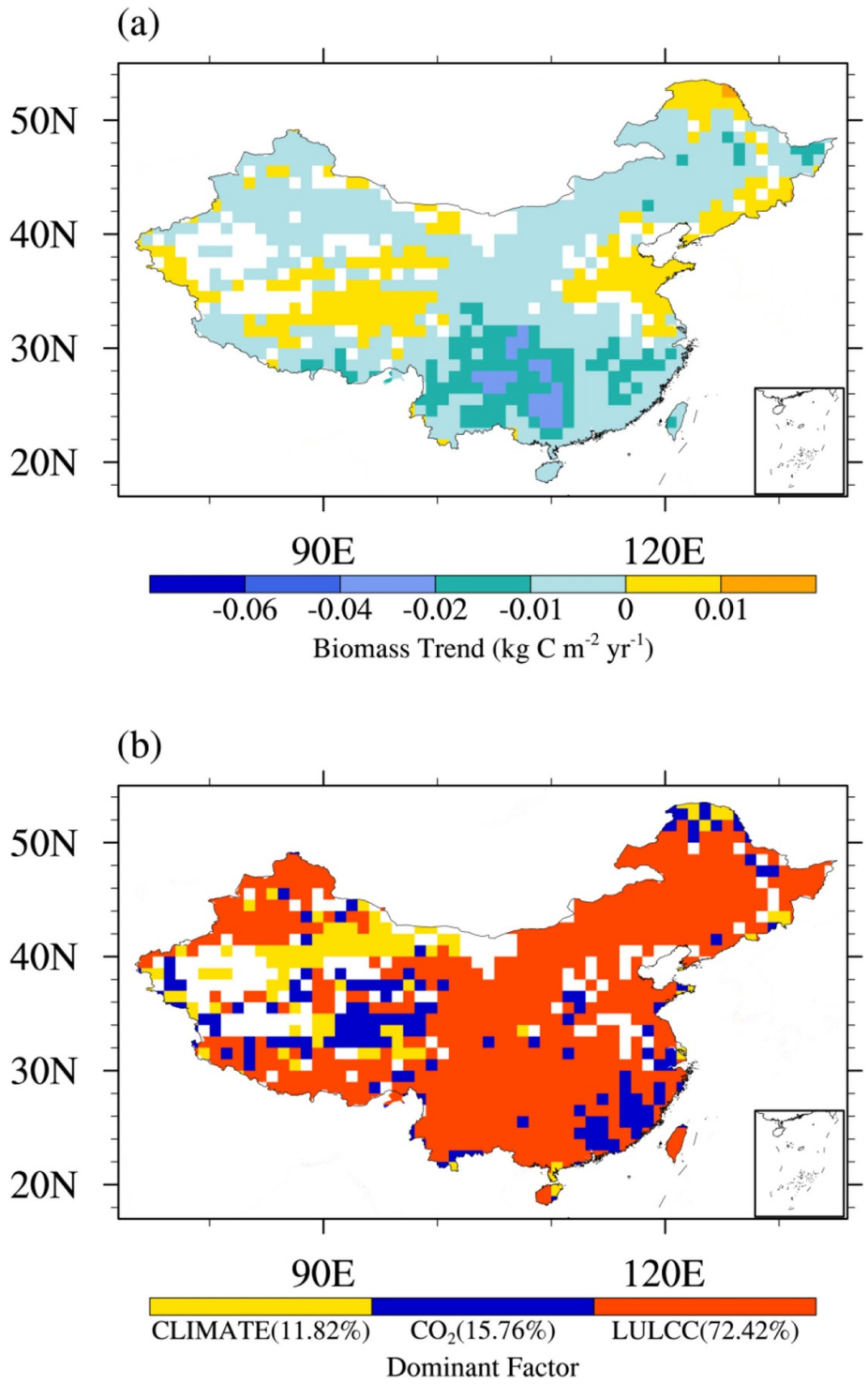

Figure 5. Spatial patterns of (a) the 20th century trend in vegetation biomass and (b) its dominant driving forcing based on bias-corrected MMEM simulations. Only grid cells that are significant at the 0.05 level using the Mann-Kendall test are shown.

to 2000, forest area in the DGVMs declined from −1.38% in JULES to −9.43% in ORCHIDEE (figure 5(a)). The areas dominated by the impact of rising [CO_2] were small, while climate change was the dominant driver for the increase in vegetation biomass only in part of northwestern China (figure 5(b)). Again, these conclusions were still robust without bias-correction, where LULCC was dominant over approximately 74.94% of China (figure S11).

4. Discussion and conclusions

Because long-term vegetation biomass observations over large regions are unavailable, DGVMs are a good choice for quantifying the trends in regional and global vegetation biomass and isolating the impacts of each driver on the scale of a century (Piao *et al* 2011). Before trend and attribution analyses, evaluation should be done and statistical or dynamical

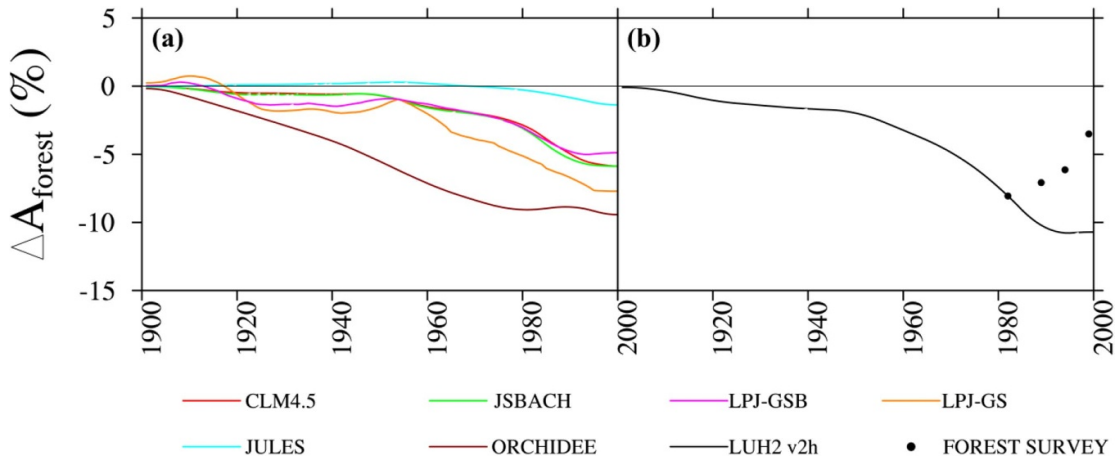

Figure 6. Changes in China's forest area percentage (ΔA_{forest}) during the 20th century over China from (a) DGVMs used in the present study based on Hurtt *et al* (2011) and from (b) LUH2_v2 h and Chinese forest survey. LULCC data from Hurtt *et al* (2011) is widely used in MIPs (e.g.FireMIP (this study), TRENDY, MsTMIP, CMIP5), LUH2_v2 h is the LULCC data for many ongoing MIPs (e.g. CMIP6, LUMIP). An 11-year running mean is used.

post-processing are often needed for the regional use of DGVM simulations because many parameters are global constants and some schemes are not optimized to fit the region of focus (Oleson *et al* 2013). Our evaluation results showed that the DGVMs often overestimated the amount of vegetation biomass in China and underestimated the spatial heterogeneity of vegetation biomass for tree and grass PFTs. The overestimation in China's vegetation biomass is partly due to underestimated turnover rate and overestimated photosynthesis for the DGVMs (table S3, supplement C) as well as overestimated forest area by 12.2% for LPJ-GS. The underestimation in spatial heterogeneity of vegetation biomass for a PFT is likely because the DGVMs generally do not consider the diversity in plant traits and individual growth within a PFT (Scheiter *et al* 2013).

To reduce the bias in DGVM simulations, machine learning GPR was used as bias-correction method. The bias-corrected DGVM simulations were much more skillful, and could simulate China's vegetation biomass reasonably well and reduced the uncertainty in DGVM simulations (smaller inter-model spread). This shows how statistical bias-correction can be used as the post-processing of model outputs to improve simulation skill and increase the reliability of subsequent quantification of temporal and spatial changes in terrestrial ecosystems. This method of bias-correction could also be applied to simulations of future changes in the vegetation biomass of China. Providing there are sufficient observations, it would be possible to use GPR bias-correction in other regions or for other simulated variables.

Our results also showed that China's vegetation biomass decreased over the 20th century with significant trend of −17.74 (−32.48 to −11.10) Tg C yr^{-1}. This is consistent with the results from Wang *et al* (2007) based on the InTEC model, but disagrees with the simulated increase of 0.02 Pg C yr^{-1} by Mao *et al* (2009) based on a version of SDGVM. The discrepancy is primarily because Mao *et al* (2009) did not account for the impact of LULCC, which we have shown is the main driver of the decrease in vegetation biomass over the century.

LULCC datasets showed that China's forest area had declined overall during the 20th century (Houghton and Hackler 2003, Hurtt *et al* 2011, Lawrence *et al* 2016). Fang *et al* (2018) estimated that vegetation carbon density for forests is > 5 times of other functional types in China based on field observation campaigns. Together, they supported our conclusions that vegetation biomass had decreased over the 20th century and LULCC was the main driver for this decrease.

Sensitivity experiments in which single factors were held constant, as here, are a commonly-used approach to isolate the impact of a forcing (e.g. Gedney *et al* 2006, Andela *et al* 2017, Erb *et al* 2018, Li *et al* 2019) but do not allow potential interactions between different drivers to be identified. Four additional sensitivity experiments, including no change in all drivers, no CO_2 and land cover change, no climate and CO_2 change, no CO_2 and climate change, would facilitate a more comprehensive attribution analysis in the next phase of FireMIP (i.e. total n^2-1 simulations, n is the number of drivers).

However, our bias correction still has limitations. First, the machine learning GPR is a statistical method and has the common problem that assumes the statistical relationship between dependent variables and independent variables (multi-year average of DGVM simulations and field observations in this study) to be constant. Second, although the field data that we collected and used had been quality controlled, they still included uncertainty and possibly errors due to sampling design, measurement techniques, and

observer bias. Such uncertainty and errors were not taken into account in our bias-correction, and may affect our estimation of trends in China's vegetation biomass. In addition, the field data used in this study represented multi-year averages and did not provide information on temporal change, so the coefficients of bias-correction models were based on multi-year averages. That is, this study just corrected the multi-year amounts and spatial pattern, which would affect our trend estimates. Long-term field measures which could provide information on temporal change are needed to improve bias-correction further and our quantitative understanding of large-scale and long-term changes in vegetation carbon pool and their drivers.

Our estimated decline in vegetation biomass after ~1980 is likely incorrect. It is not consistent with earlier studies based on Chinese forest inventory data (Fang *et al* 2001, 2007) which reported an increase in vegetation biomass from 1981 to 2000. This opposite trend is mainly because the opposite change in China's forest area used by these studies. The Chinese forest inventory data, also reported in Food and Agriculture Organization of the United Nations (FAO) national-level forest resource assessment, shows a sharp rise in China's forest area due to reforestation policy since ~1980 s (figure 6(b)) (Li and Li 1996, Ma *et al* 1997, State Administration of Forestry and Grassland 2017). However, in this study, the change in China's forest area in the DGVMs, except for ORCHIDEE whose forest area change was constrained by Houghton *et al* (2012), was characterized by a decrease after 1980 (figure 6(a)). The FireMIP models used the cropland and/or pasture area changes from Hurtt *et al* (2011), and prescribed or modeled the changes in tree, grass, and or shrub PFTs areas which shared the remaining grid area after assigning areas for water/ice/urban (constant) and cropland/pasture (prescribed), an approach widely used in international MIPs, e.g. TRENDY (Sitch *et al* 2015), MsTMIP (Ito *et al* 2016), CMIP5 (Taylor *et al* 2012). The Hurtt *et al* (2011) land use harmonization (LUH) model used inputs from HYDE 3.1 which showed an evident increase in China's cropland area in recent decades that was incorrect (Liu and Tian 2010, Zhao and Zhang 2013). With the incorrect cropland area change, China's forest area is decreased in the LULCC of Hurtt *et al* (2011) and thus models in a variety of MIPs. A sharp decrease for the 1980 s and overall constant for the 1990 s in China's forest area are also shown in LUH2_v2 h (figure 6(b)) (Lawrence *et al* 2016), that is the LULCC input data for many ongoing MIPs, e.g., CMIP6 as a basis for the next Intergovernmental Panel on Climate Change Assessment Report (IPCC AR6) (Eyring *et al* 2016). Given the importance of forest area change in simulated vegetation biomass change verified in the present study, the use of incorrect LULCC data will result in inaccurate simulation of the carbon sink and source in China for the last two decades of the 20th century in these MIPs. Therefore, the Chinese forest inventory data, and satellite-based land cover change data from Song *et al* (2018) are recommended to LUH group for improving the accuracy of LULCC and thus simulations of various MIPs and IPCC reports.

Data availability

All DGVM simulations (both uncorrected and corrected) and field observations used in this study are publicly available at http://doi.org/10.5281/zenodo.3678535 (doi: 10.5281/zenodo.3678535) and Supplement B, respectively.

Acknowledgments

This study is co-supported by the National Key Research and Development Program of China (2017YFA0604804 and 2017YFA0604302) and National Natural Science Foundation of China (41475099 and 41630530). We thank Sam Levis for revising language errors in the manuscript, and Joe Melton, Ruxu Lian, and Zhongda Lin for helpful discussions. We are also grateful to two anonymous reviewers for their valuable comments and suggestions and ERL editors for handing this paper. SPH acknowledges the support from the ERC-funded project GC2.0 (694481) and from the High-end Foreign Expert Programme of China (GDW20191100161). And acknowledge support from the Helmholtz Foundation and its ATMO programme and Impulse and Networking fund. GL is funded by the Deutsche Forschungsgemeinschaft (DFG, German Research Foundation) (338130981). Jian Ni is funded by National Natural Science Foundation of China (31870462).

ORCID iDs

Fang Li https://orcid.org/0000-0002-3686-2257
Matthew Forrest https://orcid.org/0000-0003-1858-3489

References

Ahlström A, Schurgers G, Arneth A and Smith B 2012 Robustness and uncertainty in terrestrial ecosystem carbon response to CMIP5 climate change projections *Environ. Res. Lett.* **7** 044008–10

Andela N, Morton D C, Giglio L, Chen Y and Randerson J T 2017 A human-driven decline in global burned area *Science* **356** 1356

Best M J *et al* 2011 The Joint UK Land Environment Simulator (JULES), model description-Part 1: energy and water fluxes *Geosci. Model Dev.* **4** 677–99

Brovkin V *et al* 2013 Effect of anthropogenic land-use and land-cover changes on climate and land carbon storage in CMIP5 projections for the twenty-first century *J. Climate* **26** 6859–81

Carvalhais N *et al* 2014 Global covariation of carbon turnover times with climate in terrestrial ecosystems *Nature* **514** 213–7

Chen Y Y *et al* 2016 Evaluating the performance of land surface model ORCHIDEE-CAN v1.0 on water and energy flux estimation with a single-and multi-layer energy budget scheme *Geosci. Model. Dev.* **9** 2951–72

Clark D B *et al* 2011 The Joint UK Land Environment Simulator (JULES), model description– part 2: carbon fluxes and vegetation dynamics *Geosci. Model Dev.* **4** 701–22

Erb M P, Jackson C S, Broccoli A J, Lea D W, Valdes P J, Crucifix M and Dinezio P N 2018 Model evidence for a seasonal bias in Antarctic ice cores *Nat. Commun.* **9** 1361

Eyring V, Bony S, Meehl G A, Senior C A, Stevens B, Stouffer R J and Taylor K E 2016 Overview of the Coupled Model Intercomparison Project Phase 6 (CMIP6) experimental design and organization *Geosci. Model Dev.* **9** 1937–58

Fang J Y, Chen A P, Peng C H, Zhao S Q and Ci L J 2001 Changes in forest biomass carbon storage in China between 1949 and 1998 *Science* **292** 2320–2

Fang J Y, Guo Z D, Piao S L and Chen A P 2007 Terrestrial vegetation carbon sinks in China, 1981-2000 *Sci. China* D **50** 1341–50

Fang J Y, Yu G R, Liu L L, Hu S J and Chapin III F S 2018 Climate change, human impacts, and carbon sequestration in China *Proc. Natl Acad. Sci. USA* **115** 4015–20

Foley J A, Prentice I C, Ramankutty N, Levis S, Pollard D, Sitch S and Haxeltine A 1996 An integrated biosphere model of land surface processes, terrestrial carbon balance, and vegetation dynamics *Global Biogeochem Cycles* **10** 603–28

Gedney N, Cox P M, Betts R A, Boucher O, Huntingford C and Stott P A 2006 Detection of a direct carbon dioxide effect in continental river runoff records *Nature* **439** 835–8

Hantson S *et al* 2016 The status and challenge of global fire modelling *Biogeosciences* **13** 3359–75

Hantson S *et al* 2019 Quantitative assessment of fire and vegetation properties in historical simulations with fire-enabled vegetation models from the FireMIP intercomparison project *Geosci. Model Dev.* Submitted

Houghton R A and Hackler J L 2003 Sources and sinks of carbon from land-use change in China *Global Biogeochem. Cy.* **17** 1034

Houghton R A, House J I, Pongratz J, Van der Werf G R, Defries R S, Hansen M C, Le Quéré C and Ramankutty N 2012 Carbon emissions from land use and land-cover change *Biogeosciences* **9** 5125–42

Hurtt G C *et al* 2011 Harmonization of land-use scenarios for the period 1500–2100: 600 years of global gridded annual land-use transitions, wood harvest, and resulting secondary lands *Clim. Change* **109** 117–61

Ichii K, Kondo M, Okabe Y, Ueyama M, Kobayashi H, Lee S-J, Saigusa N, Zhu Z and Myneni B R 2013 Recent changes in terrestrial gross primary productivity in Asia from 1982 to 2011 *Remote Sens.* **5** 6043–62

Ito A *et al* 2016 Decadal trends in the seasonal-cycle amplitude of terrestrial CO_2 exchange resulting from the ensemble of terrestrial biosphere models *Tellus* B **68** 28968

Keenan T F, Hollinger D Y, Bohrer G, Dragoni D, Munger J W, Schmid H P and Richardson A D 2013 Increase in forest water-use efficiency as atmospheric carbon dioxide concentrations rise *Nature* **499** 324–7

Kim J S, Kug J S and Jeong S J 2017 Intensification of terrestrial carbon cycle related to El Nino-Southern Oscillation under greenhouse warming *Nat. Commun.* **8** 1674

Klein Goldewijk K, Beusen A, van Drecht G and de Vos M 2011 The HYDE 3.1 spatially explicit database of human-induced global land-use change over the past 12,000 years *Global Ecol. Biogeogr.* **20** 73–86

Klein Goldewijk K and Verburg P H 2013 Uncertainties in global-scale reconstructions of historical land use: an illustration using the HYDE data set *Landscape Ecol.* **28** 861–77

Knorr W, Jiang L and Arneth A 2016 Climate, CO_2 and human population impacts on global wildfire emissions *Biogeosciences* **13** 267–82

Kondo M, Ichii K, Ueyama M, Mizoguchi Y, Hirata R and Saigusa N 2013 The role of carbon flux and biometirc observations in constraining a terrestrial ecosystem model: a case study in disturbed forests in East Asia *Ecol. Res.* **28** 893–905

Krinner G, Viovy N, de Noblet-ducoudré N, Ogée J, Polcher J, Friedlingstein P, Ciais P, Sitch S and Prentice I C 2005 A dynamic global vegetation model for studies of the coupled atmosphere-biosphere system *Global Biogeochem. Cy.* **19** GB1015

Lasslop G, Thonicke K and Kloster S 2014 SPITFIRE within the MPI Earth system model: model development and evaluation *J. Adv. Model. Earth Syst.* **6** 740–55

Lawrence D W *et al* 2016 The Land Use Model Intercomparison Project (LUMIP) contribution to CMIP6: rationale and experimental design *Geosci. Model Dev.* **9** 2973–98

Le Quéré C *et al* 2014 Global carbon budget 2013 *Earth Syst. Sci. Data* **6** 235–63

Lehsten V, Tansey K, Balzter H, Thonicke K, Spessa A, Weber U, Smith B and Arneth A 2009 Estimating carbon emissions from African wildfires *Biogeosciences* **6** 349–60

Li F, Levis S and Ward D S 2013 Quantifying the role of fire in the Earth system – Part 1: Improved global fire modeling in the Community Earth System Model (CESM1) *Biogeosciences* **10** 2293–314

Le Quéré C *et al* 2014 Global carbon budget 2013 *Earth Syst. Sci. Data* **6** 235–63

Li F, Zeng X D and Levis S 2012 A process-based fire parameterization of intermediate complexity in a Dynamic Global Vegetation Model *Biogeosciences* **9** 2761–80

Li F and Lawrence D M 2017 Role of fire in the global land water budget during the 20th century through changing ecosystems *J. Clim.* **30** 1893–908

Li F *et al* 2019 Historical (1700–2012) Global multi-model estimates of the fire emissions from the fire Modeling Intercomparison Project (FireMIP) *Atmos. Chem. Phys.* **19** 12545–67

Li K R, Wang S Q and Cao M K 2004 Vegetation and soil carbon storage in China *Sci. China Earth Sci.* **47** 49–57

Li N, Xie G D, Zhang C S, Xiao Y, Zhang B, Chen W H, Sun Y Z and Wang S 2015 Biomass resources distribution in the terrestrial ecosystem of China *Sustainability* **7** 8548–64

Li W H and Li F 1996 *Research on Forest Resources in China* (Beijing: China Forestry Publish House) pp 13–14 (in Chinese)

Liu M L and Tian H Q 2010 China's land cover and land use change from 1700 to 2005: estimations from high-resolution satellite data and historical archives *Global Biogeochem. Cy.* **24** GB3003

Luo T X 1996 Patterns of net primary productivity for Chinese major forest types and their mathematical models *PhD Dissertation* Chinese Academy of Sciences p 230 (in Chinese)

Ma Z L, Song C S and Zhang Q H 1997 *The Changes of Forest Distribution in China* (Beijing: China Forestry Publishing House) pp 12–60 (in Chinese)

Mangeon S, Voulgarakis A, Gilham R, Harper A, Sitch S and Folberth G 2016 INFERNO: a fire and emissions scheme for the UKMet Office's Unified Model *Geosci. Model Dev.* **9** 2685–700

Mao J F, Wang B and Dai Y J 2009 Sensitivity of the carbon storage of potential vegetation to historical climate variability and CO_2 in continental China *Adv. Atmos. Sci.* **26** 87–100

Ni J 2001 Carbon storage in terrestrial ecosystems of China: estimates at different spatial resolutions and their responses to climate change *Clim. Change* **49** 339–58

Norby R J *et al* 2005 Forest response to elevated CO_2 is conserved across a broad range of productivity *PNAS* **102** 18052–6

Oleson K W *et al* 2013 *Technical Description of Version 4.5 Of the Community Land Model (CLM)* (NCAR/TN-503+STR) (USA: NCAR Boulder)

Pan Y D, Luo T X, Birdsey R, Hom J and Melillo J 2004 New estimations of carbon storage and sequestration in China's forests: effects of age-class and method on inventory-based carbon estimation *Clim. Change* **67** 211–36

Piao S L *et al* 2011 Contribution of climate change and rising CO_2 to terrestrial carbon balance in East Asia: A multi-model analysis *Global Planet. Change* **75** 133–42

Rabin S S *et al* 2017 The Fire Modeling Intercomparison Project (FireMIP), phase 1: experimental and analytical protocols with detailed model descriptions *Geosci. Model Dev.* **10** 1175–97

Reick C H, Raddatz T, Brovkin V and Gayler V 2013 Representation of natural and anthropogenic land cover change in MPI-ESM *J. Adv. Model. Earth Syst.* **5** 459–82

Scheiter S, Langan L and Higgins S I 2013 Next-generation dynamic global vegetation models: learning from community ecology *New Phytol.* **198** 957–69

Sitch S *et al* 2003 Evaluation of ecosystem dynamics, plant geography and terrestrial carbon cycling in the LPJ dynamic global vegetation model *Glob. Change Biol.* **9** 161–85

Sitch S *et al* 2015 Recent trends and drivers of regional sources and sinks of carbon dioxide *Biogeosciences* **12** 653–79

Smith B, Prentice I C and Sykes M T 2001 Representation of vegetation dynamics in the modelling of terrestrial ecosystems: comparing two contrasting approaches within European climate space *Global Ecol. Biogeogr.* **10** 621–37

Smith B, Wårlind D, Arneth A, Hickler T, Leadley P, Siltberg J and Zaehle S 2014 Implications of incorporating N cycling and N limitations on primary production in an individual-based dynamic vegetation model *Biogeosciences* **11** 2027–54

Song X P, Hansen M C, Stehman S V, Potapov P V, Tyukavina A, Vermote E F and Townshend J R 2018 Global land change from 1982 to 2016 *Nature* **560** 639–43

State Administration of Forestry and Grassland 2017 *China Forestry Statistical Yearbook 2017* (Beijing: China Forestry Press) pp 396

Tang X L *et al* 2018 Carbon pools in China's terrestrial ecosystems: new estimates based on an intensive field survey *PNAS* **115** 4021–6

Taylor K E, Stouffer R J and Meehl G A 2012 An overview of CMIP5 and the experiment design *Bull. Amer. Meteor. Soc.* **93** 485–98

Wang S, Chen J M, Ju W M, Feng X, Chen M, Chen P and Yu G 2007 Carbon sinks and sources in China's forests during 1901–2001 *J. Environ. Manage.* **85** 524–37

Wilks D S 1995 *Statistical Methods in the Atmosphere Sciences: An Introduction* (New York: Academic) pp 467

Xin Q C, Dai Y J, Li X, Liu X P, Gong P and Richardson A D 2018 A steady-state approximation approach to simulate seasonal leaf dynamics of deciduous broadleaf forests via climate variables *Agr. Forest Meteorol.* **249** 44–56

Xu L, Yu G R, He N P, Wang Q F, Gao Y, Wen D, Li S G, Niu S L and Ge J P 2018 Carbon storage in China's terrestrial ecosystems: a synthesis *Sci. Rep.* **8** 2806

Yue C *et al* 2014 Modelling the role of fires in the terrestrial carbon balance by incorporating SPITFIRE into the global vegetation model ORCHIDEE—Part 1: simulating historical global burned area and fire regimes *Geosci. Model Dev.* **7** 2747–67

Yue C, Ciais P, Cadule P, Thonicke K and van Leeuwen T T 2015 Modelling the role of fires in the terrestrial carbon balance by incorporating SPITFIRE into the global vegetation model ORCHIDEE—part 2: carbon emissions and the role of fires in the global carbon balance *Geosci. Model Dev.* **8** 1321–38

Zhao L M and Zhang S H 2013 The accuracy evaluation of two common global historical land use/cover datasets in China *J. Northwest A&F Univ. (Natural Science Edition)* **41** 133–40